Light scattering spectroscopy of cells: a study based on Mie and fractal models

Tao T. Wu[a]*, Min Xu[b], and Jianan Y. Qu[a]

[a]Department of Electronic and Computer Engineering,
Hong Kong University of Science and Technology, Hong Kong, P. R. China

[b]Department of Physics, Fairfield University, Connecticut, USA

ABSTRACT

The changes in light scattering induced by acetic acid in cervical cancer cell suspensions and the attached monolayer cells were studied using elastic light scattering spectroscopy. The results show that Mie scattering is dominant in small forward scattering angles (<10.0 degrees). However Mie fitting was found not to be able to provide a satisfactory interpretation of the scattering spectral signals in the large scattering angles. This creates challenge to extract accurate information on the refractive index of cellular organelles. The internal structures in the cells do not make appreciable contribution to light scattering in the small scattering angles while these structures show up and dominate the light scattering in larger angles. The fractal mechanism captures these internal structures. After applying acetic acid solution to the cells, it was found that the volume fraction of the small size scatterers increases and the largest scatterer size decreases. Meanwhile, the fluctuation amplitude of intracellular refractive index increases. Overall, the results provide the evidence that small-sized organelles are the major contributors to the acetowhitening effect.

KEYWORDS: light scattering spectroscopy, fractal mechanism, acetowhitening

1. INTRODUCTION

Acetic acid technique which is used in colposcopy involves applying 3-5% acetic acid to the cervix to induce the acetowhitening effect and create the contrast between precancerous lesions and normal tissues. The acetowhitening phenomenon, where the abnormal tissue usually turns white while the normal tissue remains unchanged, is transient and reversible[1]. The application of acetic acid makes the optical properties of cell changed so that it increases the intensity of backscattering light. The backscattering light may contain information to distinguish the abnormal and normal cervical tissues and can be used to guide the medical diagnose in clinic. So to study the mechanism of the acetic acid and cells/tissue interaction may help us to understand what behind this acetic acid test.

In this work we used elastic light scattering spectroscopy (LSS) to investigate the changes in light scattering from cervical squamous carcinoma cell line (SiHa). The noninvasive LSS technique, an important tool to study the optical properties from cellular organelles and tissue structural features, has been investigated by a variety of groups[2-10]. It was found that the wavelength and the angular dependent backscattering spectra from tissues or cells could be interpreted by the cell and nuclear size distribution[2-4]. At the same time, Mourant et al. suggested that much of the light scattering comes from scatterers with smaller sizes, such as the small organelles or internal structures within the nucleus and cytoplasm[7]. Mie fitting was found not to be able to provide a satisfactory interpretation of scattering spectral signals, especially for the large angles[10]. The internal structures in the cells may dominate the light scattering in larger angles. Models which take into account scattering from intact cells and other cellular structures are necessary to be considered for understanding the phenomena of acetowhitening at cellular level.

Recently, the fractal mechanism of biological tissue and cells was investigated[11-13], where the tissue is modeled as a fractal continuous random medium. The light scattering is caused by the weak random fluctuations of the dielectric

* Corresponding Email: eewt@ust.hk

Biomedical Applications of Light Scattering, edited by Adam Wax, Vadim Backman,
Proc. of SPIE Vol. 6446, 64460H, (2007) · 1605-7422/07/$18 · doi: 10.1117/12.697141

permittivity. Good preliminary results are obtained to fit the light scattering from tissue and cells over a large scattering angle and wavelength range[13].

In this paper, a combined Mie and fractal model is proposed to study the light scattering from intact cells. The light scattering from the whole cells dominated in the forward light scattering is interpreted by Mie scattering model and the light scattering from the internal structures is fitted by fractal model. We measured the wavelength and angular dependent light scattering spectra from the intact cells. The size and refractive index of the cells and intercellular components were measured and calculated, respectively, for more accurate estimation of changes in cells before and after the application of acetic acid.

2. MATERIALS AND METHODS

2.1. Cell Cultures and Suspensions

Siha cell line from the American Type Cell Collection was used in this study. Two types of cell samples are used. One type is cell suspension and the other one is attached monolayer cells. Cell suspensions were prepared as follows. The cells were maintained in culture medium to 80% confluence in tissue culture dishes and then detached by Trypsin-EDTA solution. After the addition of the complete culture medium, the cell suspensions were centrifuged (500 g for 5 min) and then washed twice by PBS and resuspended in PBS on ice until the light scattering experiments. Attached monolayer cells were cultured on 18 x 18 mm cover glass to different confluence for the light scattering experiments.

The volumes of the cells in cell suspensions were measured by a Mutisizer II Coulter counter and verified by phase contrast microscope. The cell volume distribution was used to estimate the mean cell diameter of the cell population, which was used in the Mie calculations. Here, the size distribution of SiHa cells was described by a log-normal distribution[10].

2.2. Wavelength and Angular Dependent Light Scattering Spectrum Measurements

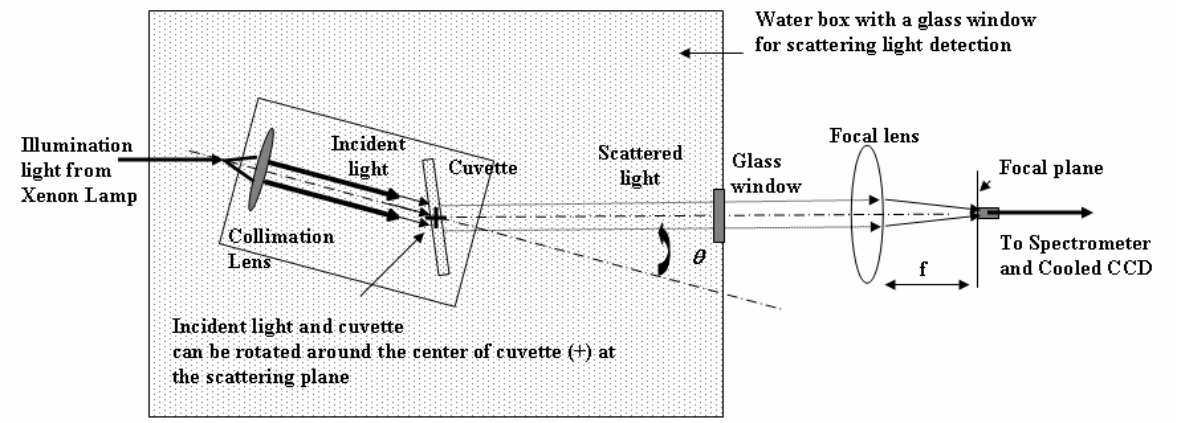

Figure 1: Schematic of the light scattering spectroscopy setup.

The system schematic for LSS measurement is shown in Fig. 1. Broadband white light from a 75W Xenon arc source was focused onto a 400 μm fiber and was then collimated by a focal lens (f = 100 mm). The cell samples are placed in a homemade cuvette (18 × 15 × 1.1 mm, width × height × thickness). The diameter of the collimated beam illuminated on the samples is about 6 mm. The scattered light at a given angle was focused by a lens of 200 mm focal length onto a 400 μm fiber and was collected by a spectrometer coupled with a cooled CCD camera. The collimation part and the cuvette were fixed on a rotation stage and immerged in a water tank. The angle θ was determined by the rotation stage with a resolution of 0.02 degree. The minimal and maximal measurement angles of the system were 0.8 and 175 degrees, respectively. The spectral resolution of our system was about 7 nm. In the measurements, the glass cuvette was tilted to 23 degrees to avoid the reflection of the unscattered light and the forward scattering on the second cuvette surface.

LSS measurements are performed on the cell suspensions diluted in PBS and PBS with acetic acid, respectively and the attached monolayer cells in culture medium and culture medium with acetic acid, respectively. To avoid multiple scattering in cells suspensions, the concentrations of cells varied from 0.1 x 10^5 to 2 x 10^5 cells/ml in all the experiments, which are consistent with the report from Mourant et al[10]. The concentration of acetic acid solution was set to 0.3% (v/v) glacial acetic acid in PBS and 0.6% in culture medium[14]. The measured scattering spectra were in the wavelength range from 400 to 700 nm and the integration time of the CCD is from 0.01 s to 1 s in the forward scattering angles and from 30 s to 100 s in the large scattering angles. The total acquisition time of the whole set of data is about 20 to 30 minutes in which period the acetowhitening signal is relatively stable.

2.3. Mie Theory and Fractal Mechanism

A Mie theory model, the homogenous sphere model, was used to fit the measured scattering spectra from the intact cells, and a fractal model was used to fit the light scattering spectra from the intracellular components, which is regarded as a continuous random media. The light scattering amplitude function is related to the correlation function of the random fluctuations of the dielectric permittivity in the media, which depends on the fractal dimension $\boldsymbol{D_f}$, the cutoff correlation length $\boldsymbol{l_{max}}$ as well as the light scattering strength $\boldsymbol{\beta}$. An exponential correlation function was considered by Moscoso *et al.*[11] for modeling tissue light scattering. Xu *et al.* assumed that the correlation function of the random fluctuations of the dielectric permittivity, in the fractal continuous medium model, is an average of exponential functions weighted by power law distribution[13]. Therefore, the amplitude scattering function $\boldsymbol{S(\theta)}$ can now be written as[13]:

$$\left|\boldsymbol{S}(\boldsymbol{\theta})\right|^2 = \boldsymbol{\beta}^2 \int_0^{\boldsymbol{kl}_{\max}} \frac{\boldsymbol{k}^{\boldsymbol{D_f}-1}\boldsymbol{x}^{6-\boldsymbol{D_f}}}{\left[1+2(1-\cos\boldsymbol{\theta})\boldsymbol{x}^2\right]^2}\boldsymbol{dx} \tag{1}$$

where k is the wave number, $\boldsymbol{\beta} \propto \boldsymbol{n}_0\Delta\boldsymbol{n}$, $\boldsymbol{n}_0, \Delta\boldsymbol{n}$ are the refractive index of the background of the biological tissue and the refractive index fluctuation amplitude. The squared scattering amplitude function of whole cells can be approximated simply by:

$$\left|\boldsymbol{S}_{\boldsymbol{Cell}}(\boldsymbol{\theta},\boldsymbol{\lambda})\right|^2 = \left|\boldsymbol{S}_{\boldsymbol{Mie}}(\boldsymbol{\theta},\boldsymbol{\lambda})\right|^2 + \left|\boldsymbol{S}_{\boldsymbol{Fractal}}(\boldsymbol{\theta},\boldsymbol{\lambda})\right|^2 \tag{2}$$

Based on the Mie and fractal model, we calculated the wavelength and angular dependent scattering spectra along the scattering plane from the scatterers. The light scattering spectra were calculated based on the codes from Wiscombe[15] and the formula of fractal model[13]. The spectral data were fitted over the wavelength region of 400 to 700 nm by minimizing the function

$$\boldsymbol{\chi}^2 = \sum_1^{\boldsymbol{n_\theta}}\sum_1^{\boldsymbol{n_w}}\left\{\left[\log\left(\boldsymbol{I}^c(\boldsymbol{\lambda},\boldsymbol{\theta})\right)-\log\left(\boldsymbol{I}^e(\boldsymbol{\lambda},\boldsymbol{\theta})\right)\right]^2 / \log\left(\boldsymbol{I}^e(\boldsymbol{\lambda},\boldsymbol{\theta})\right)\right\} \tag{3}$$

where $I^c(\lambda,\theta)$ and $I^e(\lambda,\theta)$ were the calculated and experiment spectra at different wavelengths and angles, respectively. $\boldsymbol{n_w}$ and $\boldsymbol{n_\theta}$ represent the number of wavelengths and angles used in the fitting function, respectively.

3. RESULTS AND DISSCUTION

3.1. Calibration of LSS Measurements and Mie Fitting

Polystyrene spheres of 6.14 μm in diameter were used to verify the light scattering measurement setting and the Mie calculations. The empirical equation for the refractive index of the microspheres is

$$\boldsymbol{n} = \boldsymbol{a} + \boldsymbol{b}/\boldsymbol{\lambda}^2 \tag{4}$$

where $\boldsymbol{a}$ and $\boldsymbol{b}$ are fitting parameters and $\boldsymbol{\lambda}$ is the wavelength[16]. In the Mie fitting, Eq. (4) was used for the refractive index of the microspheres and the wavelength dependent refractive index of distilled water was taken from Ref. [17]. The light scattering spectra of the microspheres suspensions at different angles could be well globally fitted by the Mie fitting. From the fitting, a mean particle size of 5.95 μm with a standard deviation of 0.03 μm was achieved, which is within the manufacturer's precision measurements. We show the angular dependent spectrum in Fig. (2). The intensity in the figure is the integrated intensity from the wavelength 400 – 700 nm.

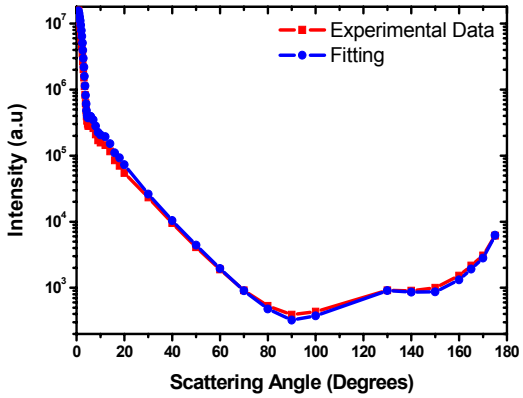

Figure 2: Light scattering spectra and the best fitting for polystyrene spheres.

3.2. Light Scattering from Cell Suspensions

Mie theory provides good interpretation of LSS signals from the scattering from spherical particles. Therefore, the cell suspensions were used in LSS measurements because most cells in suspension are almost spherically shaped.

The angular dependent light scattering spectra from the cell suspension before and after the application of acetic acid at multiple scattering angles are shown in Fig. 3. The spectrum and intensity changes before and after adding acetic acid were small in the small scattering angles. When the scattering angle was larger than 5.0 degrees, the intensity increases by about 5-9 times after adding acetic acid, as shown in Fig. 3(a, b). The scattering spectrum is an almost linear decay from 400 to 700 nm. The scattering oscillation pattern presented in the small scattering angles disappears in the large scattering angles. It is because that the light scattering from the small-sized cellular components becomes larger. The scattering from small-sized scatterers are more angularly isotropic and decay monotonically in wavelength domain. Though the Mie scattering of the cell and nucleus dominate the signals in the small angles, it may be overwhelmed by the scattering of small-sized scatterers in large angles.

Wavelength and angular dependent light scattering data from intact cell suspension were fitted with the combined Mie and fractal model, as described in the materials and methods section. The diameter of the cells in the suspension before and after the application of acetic acid was $\phi = 14.00 \pm 1.75$ and $\phi' = 15.20 \pm 1.75$ μm, respectively. In our fittings, the cell refractive index was described by Eq. (4). The refractive index of the PBS (culture medium) and the acetic acid solution was calculated using the empirical equation for the refractive index of distilled water[17]. We used the Eq. (1) to calculate the scattering amplitude of the small components and fine structures in the intact cells. The fractal dimension D_f, the cutoff correlation length l_{max} and the light scattering strength β were the fitting parameters to obtain the best fitting.

In the small scattering angles, the Mie model scattering dominates the scattering spectrum while in the large scattering angles, the fractal model scattering dominates the scattering spectrum. Fig. 3 shows the angular fitting results on the light scattering spectra from cell suspensions before (a) and after (b) the application of acetic acid. The fitting results are good for most of the angles. The Mie model can fit the light scattering spectra at the forward scattering angles (< 10 degrees) and the fractal model can fitting the spectra at the larger scattering angles. However, we found that the homogeneous sphere model could not achieve very good global fitting to the measured scattering spectra at all the small scattering angles because the content of the cell is not homogenous, the organelles in a cell contribute to the light scattering and distort the scattering spectrum of the whole cell, the assumed homogenous spherical particle.

The fitting parameters are listed in table 1. We can find that the mean refractive index of the cell reduces due to the increase of the cell size after the application of acetic acid. The fractal dimension D_f increases a little which means that the volume fraction of the small size scatterers in the cells increases. From the cutoff correlation length l_{max} we can find that the largest scatterer's size decreases. From the parameter β we can know that fluctuation amplitude of intracellular refractive index increases about 2.49 times so that more light are scattered in the large scattering angles.

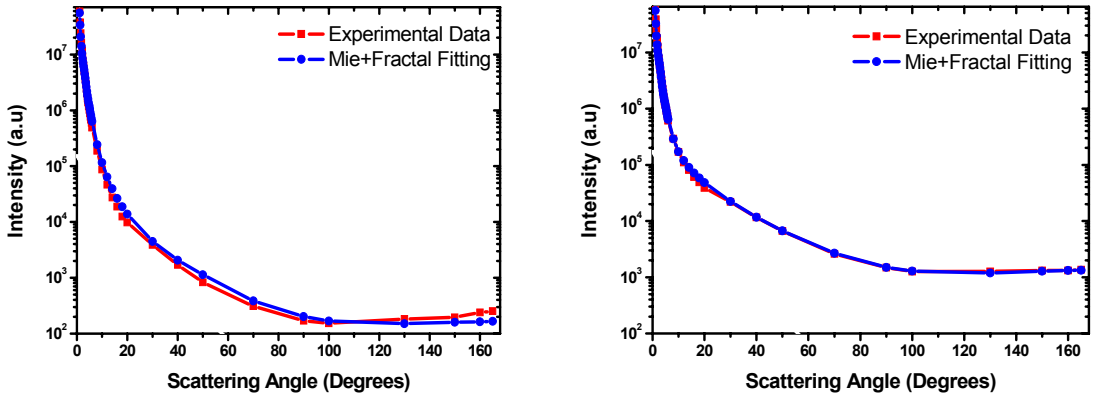

(a) (b)

Figure 3: Light scattering spectra of cells before (a) and after (b) the application of acetic acid with the best fitting. The intensity is the integrated intensity from the wavelength 400 – 700 nm.

Table 1. The parameters in the Mie and fractal fitting.

	Cell Suspension		Monolayer Cells
	Mie	Fractal	Fractal
Before AA	$n_{Cell} = 1.3503 + 4433/\lambda 2$ $\phi = 14.0 \pm 1.75\ \mu m$	$D_f = 4.53$ $l_{max} = 0.52$ $\beta = 109.24$	$D_f = 4.49$ $l_{max} = 0.87$ $\beta = 357.15$
After AA	$n'_{Cell} = 1.3469 + 4673/\lambda 2$ $\phi' = 15.2 \pm 1.75\ \mu m$	$D_f' = 4.61$ $l_{max}' = 0.24$ $\beta' = 271.92$	$D_f' = 4.88$ $l_{max}' = 0.73$ $\beta' = 505.51$
$\frac{\Delta n_2}{\Delta n_1}$	----	2.49	1.42

3.3. Light Scattering from Attached Monolayer Cells

The wavelength and angular dependent light scattering spectra from the attached monolayer cells before and after the application of acetic acid were also measured using LSS. Similar to the cell suspensions, the light scattering spectra of attached monolayer cells are with some oscillation pattern in the small scattering angles and then become a monotonic decay with the increase of wavelength when the angle is larger than 3 degrees. The intensity change is small at the small scattering angles and is 5-9 times in the larger scattering angles. We only show the angular dependent light scattering spectrum from 100% confluence attached monolayer cells in Fig. 4.

Since the shape of the attached monolayer cells is irregular we only use the fractal model to fit the spectra from 10 degrees. A good global fitting can be achieved for both the spectra before and after the application of acetic acid. The fitted spectra and fitting parameters are shown in Fig. 4 and table 1. Again, the volume fraction of the small size scatterers increases; the largest scatterer's size decreases; and the fluctuation amplitude of intracellular refractive index increases about 1.42 times.

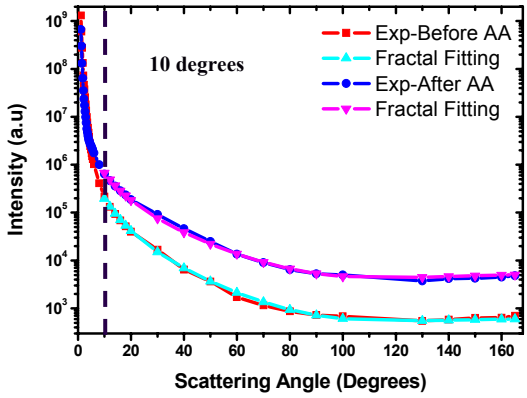

Figure 4: Light scattering from attached monolayer cells with the fractal model fitting from 10 degrees. The intensity is the integrated intensity from the wavelength 400 – 700 nm.

We found that the light scattering characteristics in large scattering angles does not strongly depend on the confluence of the monolayer cells which means almost all the light is scattered from the intracellular components in the large angles. In the small scattering angles (< 3 degrees), the scattering pattern is a little changed which demonstrates that the higher confluence the monolayer cells, the smaller the scatterer diameter if we apply Mie theory to fit the small angle scattering spectra. This may be explained that the diameter of the nucleus will be decreased when the monolayer cells are crowed.

4. CONCLUSION

The scattering spectra measured from the cell suspensions and the attached monolayer cells show that the acetic acid-induced change is very small in the forward scattering angles. But in the large scattering angles, acetic acid induces great increase in the intensity of scattered light. The scattering characteristics of the cells in both types have some Mie-Fractal duality. Mie scattering is dominant in small forward scattering angles (< 10.0 degrees) and the contributions from fractal scatterings of the fine structures in cells become significant when the scattering angle is greater.

Combined Mie and fractal model provides good global-fitting of the scattering spectra measured from cell suspension and attached monolayer cell cultures. After the application of acetic acid, both relative weight of small scattering structure and fluctuation amplitude of intracellular refractive index increases which contribute to 5-9 times increase of large angle scattering. The results provide the evidence that small-sized organelles are the major contributors to the acetowhitening effect.

The authors acknowledge support from the Hong Kong Research Grants Council through grants HKUST6052/00M and HKUST6025/02M.

REFERENCES

1. M. C. Anderson, J. A. Jordan, A. R. Morse, and F. Sharp, *A Text and Atlas of Integrated Colposcopy: for Colposcopists, Histopathologists and Cytologists* (Chapman & Hall Medical, London, 1992).
2. L. T. Perelman, V. Backman, M. Wallace, G. Zonios, R. Manoharan, A. Nusrat, S. Shields, M. Seiler, C. Lima, T. Hamano, I. Itzkan, J. Van Dam, J. M. Crawford, M. S. Feld, "Observation of periodic fine structure in reflectance from biological tissue: a new technique for measuring nuclear size distribution," Phys. Rev. Lett. **80**, 627-630 (1998).
3. V. Backman, R. Gurjar, K. Badizadegan, R. Dasari, I. Itzkan, L. T. Perelman, M. S. Feld, "Polarized light scattering spectroscopy for quantitative measurement of epithelial cellular structures in situ," IEEE J. Sel. Top. Quant. Elect. **5**, 1019-1026 (1999).
4. A. Wax, C. Yang, V. Backman, K. Badizadegan, C. W. Boone, R. R. Dasari, M. S. Feld, "Cellular organization and substructure measured using angle-resolved low-coherence interferometry," Biophys. J. **82,** 2256-2264 (2002).

5. K. Sokolov, R. Drezek, K. Gossage, and R. Richards-Kortum, "Reflectance spectroscopy with polarized light: is it sensitive to cellular and nuclear morphology?" Opt. Express **5**, 302-317 (1999).
6. J. D. Wilson and T. H. Foster, "Mie theory interpretations of light scattering from intact cells," Opt. Lett. **30**, 2442-2444 (2005).
7. J. R. Mourant, J. P. Freyer, A. H. Hielscher, A. A. Eick, D. Shen, and T. M. Johnson, "Mechanisms of light scattering from biological cells relevant to noninvasive optical tissue diagnostics," Appl. Opt. **37**, 3586-3593 (1998).
8. R. Drezek, A. Dunn, and R. Richards-Kortum, "A pulsed finite-difference time-domain (FDTD) method for calculating light scattering from cells over broad wavelength ranges," Opt. Express **6**, 147-157 (2000).
9. J. D. Wilson, C. E. Bigelow, D. J. Calkins, and T. H. Foster, "Light scattering from intact cells reports oxidative-stress-induced mitochondrial swelling," Biophys. J. **88**, 2929-2938 (2005).
10. J. R. Mourant, T. M. Johnson, S. Carpenter, A. Guerra, T. Aida, and J. P. Freyer, "Polarized angular dependent spectroscopy of epithelial cells and epithelial cell nuclei to determine the size scale of scattering structures," J. Biomed. Opt. **7**, 378–387 (2002).
11. M. Moscoso, J. B. Keller, and G. Papanicolaou, "Depolarization and blurring of optical images by biological tissue," J. Opt. Soc. Am. A **18**, 948-960 (2001).
12. J. M. Schmitt and G. Kumar, "Optical Scattering Properties of Soft Tissue: A Discrete Particle Model," Appl. Opt. **37**, 2788-2797 (1998).
13. M. Xu and R. R. Alfano, "Fractal mechanisms of light scattering in biological tissue and cells," Opt. Lett. **30**, 3051-3053 (2005).
14. T. T. Wu, J. Y. Qu, T. H. Cheung, S. F. Yim, and Y. F. Wong, "Study of dynamic process of acetic acid induced-whitening in epithelial tissues at cellular level," Opt. Express **13**, 4963-4973 (2005).
15. W. J. Wiscombe, "Improved Mie scattering algorithms," Appl. Opt. **19**, 1505-1509 (1980).
16. E. Marx and G. W. Mulholland, "Size and refractive index determination of single polystyrene spheres," J. Res. Natl. Bur. Stand. **88**, 321-338 (1983).
17. International Association for the Properties of Water and Steam, "Release on the refractive index of ordinary water substance as a function of wavelength, temperature and pressure," (1997), http://www.iapws.org/relguide/rindex.pdf.